

GLOBAL LIFETIME MEASUREMENTS OF
HIGHLY-DEFORMED AND OTHER ROTATIONAL
STRUCTURES IN THE A~135 LIGHT RARE-EARTH
REGION: PROBING THE SINGLE-PARTICLE MOTION
IN A ROTATING POTENTIAL*

M.A. RILEY,¹ R.W. LAIRD,¹ F.G. KONDEV,^{1,12} D.J. HARTLEY,^{1,7} D.E.
ARCHER,^{1,13} T.B. BROWN,¹ R.M. CLARK,² M. DEVLIN,³ P. FALLON,²
I.M. HIBBERT,⁴ D.T. JOSS,⁵ D.R. LAFOSSE,³ P.J. NOLAN,⁵ N.J.
O'BRIEN,⁴ E.S. PAUL,⁵ J. PFOHL,¹ D.G. SARANTITES,³ R.K.
SHELINE,¹ S.L. SHEPHERD,⁵ J. SIMPSON,⁶ R. WADSWORTH,⁴ M.T.
MATEV,⁷ A.V. AFANASJEV,^{8,15} J. DOBACZEWSKI,^{9,10} G.A.
LALAZISSIS,^{8,10,14} W. NAZAREWICZ,^{7,9,11} AND W. SATUŁA^{9,10}

¹Department of Physics, Florida State University, Tallahassee, FL 32306

²Nuclear Science Division, Lawrence Berkeley National Lab., Berkeley, CA 94720

³Department of Chemistry, Washington University, St. Louis, MO 63130

⁴Department of Physics, University of York, Heslington, York YO1 5DD, UK

⁵Oliver Lodge Laboratory, University of Liverpool, Liverpool L69 3BX, UK

⁶CLRC, Daresbury Laboratory, Daresbury, Warrington, WA4 4AD, UK

⁷Dept of Physics and Astronomy, Univ. of Tennessee, Knoxville, TN 37996

⁸Physik-Dept der Technischen Universität München

D-85747, Garching, Germany

⁹Institute of Theoretical Physics, Warsaw University

ul. Hoża 69, PL-00681 Warsaw, Poland

¹⁰Joint Institute for Heavy Ion Research, Oak Ridge National Laboratory

P.O. Box 2008, Oak Ridge, TN 37831

¹¹Physics Division, Oak Ridge National Laboratory, P.O. Box 2008, Oak Ridge,

TN 37831

¹²Physics Division, Argonne National Laboratory, Argonne, IL 60439

¹³Lawrence Livermore National Laboratory, Livermore, CA 94550

¹⁴Department of Theoretical Physics, Aristotle University of Thessaloniki,

Gr-54006 Thessaloniki, Greece

¹⁵ Laboratory of Radiation Physics, Institute of Solid State Physics, University of

Latvia, LV 2169 Salaspils, Miera str. 31, Latvia

* Invited talk presented at the "High Spin Physics 2001" NATO Advanced Research Workshop, dedicated to the memory of Zdzisław Szymański, Warsaw, Poland, February 6–10, 2001

It has been possible, using GAMMASPHERE plus Microball, to extract differential lifetime measurements free from common systematic errors for over 15 different nuclei (various isotopes of Ce, Pr, Nd, Pm, and Sm) at high spin within a single experiment. This comprehensive study establishes the effective single-particle quadrupole moments in the $A \sim 135$ light rare-earth region. Detailed comparisons are made with calculations using the self-consistent cranked mean-field theory.

PACS numbers: PACS 21.10.Re, 21.10.Tg, 21.60.Gx, 23.20.Lv, 27.60.+j

1. Introduction to Nuclear Shapes

In 1936 Casimir argued that non-spherical nuclear shapes were necessary to explain the hyperfine structure seen in atomic and molecular spectra [1]. A year later Bohr and Kalckar [2] suggested that by observing the gamma-ray emissions from excited nuclei one could find out more about these shape properties. Following these pioneering suggestions, the strongly interacting aggregation of fermions in nuclei have been found to display a remarkable diversity of both static and dynamic shape phenomena (see for example References [3], [4] and [5]).

Few scientists have contributed as much to the amazing developments and excitement in our field as Szymański. I well remember the first time I heard him speak. It was at one of the famous May high spin gatherings at the Niels Bohr Institute in Risø in the early 1980's. The discussion had become somewhat bogged down on something rather trivial. It was then that Szymański rose to his feet from the back of the audience, (in a similar manner to how his mind had just "risen above the tree-line in order to see the forest") and speaking softly in his wonderful way, he was able to steer the conversation out of the "trees" and towards something much more important. So often we "regular mortals" get carried away with the little details and fail to comprehend the grand scheme or how it all fits together. Szymański clearly possessed a rare ability to see the "big picture". Amazingly, he has been able to pass this leadership gift onto his "scientific children". His achievements, and those of the Warsaw group which he created and cultivated, are legendary. He was a true "Titan" of our field!

The basic microscopic mechanism leading to the existence of deformed configurations, *spontaneous symmetry-breaking*, was first proposed by Jahn and Teller for molecules [6]. The basic element of the Jahn-Teller (JT) effect is the vibronic coupling (the JT matrix element) between the collective excitations of the system and the single-particle motion. The JT effect was brought to nuclear structure by A. Bohr in his paper on "The Coupling of Nuclear Surface Oscillations to the Motion of Individual Nucleons" [7]. In Bohr's picture, the vibronic coupling was represented by the interaction

between the single-particle motion of valence nucleons and the collective excitations (multipole vibrations) of the core, known as the particle-vibration (PV) coupling. This coupling is a central element in the analysis of nuclear collective modes and nuclear deformations [3]. Depending on the geometrical properties of the individual valence nucleon (i.e., anisotropy of its wave function), the PV coupling can result in core polarization that can change the original deformation of the core. If residual interactions are present, they effectively reduce the magnitude of the JT coupling. In particular, pairing correlations in atomic nuclei give rise to a large residual energy (energy gap) which weakens deformation effects. As a result, nuclear ground-state configurations experience weak JT (or pseudo-JT) effect; the extreme JT effect can take place in excited nuclear states such as high spin states. (See Refs. [8, 9] for more discussion of the nuclear JT effect.)

2. Nuclear Superdeformation, Rotation, and Quadrupole Moments

A stunning observation in studies of rapidly rotating atomic nuclei is that due to the strong Coriolis force residual two-body correlations (e.g., pairing) are significantly quenched at high angular momenta. Indeed, the excellent reproduction of experimental high spin data (moments of inertia, alignments, routhians) by calculations without pairing (see, e.g., Refs. [10, 11] and references quoted therein) suggests that, in the high-frequency regime, the configuration mixing due to pairing is weak. Another factor that further contributes to the diminished role of residual correlations is the reduced single-particle level density at the Fermi surface due to the presence of strong shell effects at deformed shapes. The resulting deformed potentials give rise to magic numbers that appear just as strikingly, but at quite different N and Z values, as for a spherical nucleus. Consequently, highly deformed and superdeformed bands are probably the clearest examples of a pure single-particle motion in a deformed potential [12] and wonderful laboratories of the nuclear JT effect and shape polarization.

In the $A \sim 135$ ($Z=58-62$) light rare-earth region, a variety of rotational sequences with characteristics consistent with highly-deformed prolate shapes with quadrupole deformation of $\beta_2 \sim 0.30-0.40$, compared with $\beta_2 \sim 0.20$ for normal ground state deformations, have been observed [13]. These studies have revealed that the existence of highly-deformed bands is the result of an interplay between microscopic shell effects, such as the occurrence of large shell gaps near $Z=58$ and $N=72$ in the nucleon single-particle energies, and the occupation of high- j low- Ω intruder orbitals. Initially, it was thought that the involvement of one or more $i_{13/2}$ neutrons was necessary for the strong polarization of the nuclear shape to stabilize large deformation in

this mass region [14]. However, recently it was shown that bands involving the partial de-occupation of the extruder $g_{9/2}[404]9/2$ proton orbital in the odd- Z praseodymium (see [16] and references therein) and promethium [17] isotopes also exhibit comparable quadrupole deformations [18]. Furthermore, for nuclei below $N=73$ where the occupancy of the $i_{13/2}$ neutron is energetically unfavored, there are indications that bands involving the $f_{7/2}, h_{9/2} [541]1/2$ neutron orbital may also push the nucleus to “enhanced” deformation (see [19] and references therein). (For representative single-particle diagrams, see Refs. [14, 18].) In an attempt to further understand the deformation properties of a variety of different single-particle orbitals throughout the $A\sim 135$ mass region, a comprehensive lifetime experiment with measurements on over 15 different nuclei was performed. While such an idea has been exploited for several cases in the $A=80$ [20] and 135 [21, 22] highly-deformed, and the $A=150$ [23, 24, 25] and 190 [26] superdeformed regions, it has never been done before in such a global manner.

From the measured lifetimes, one can extract “differential” transition quadrupole moments

$$\delta Q_t(^A Z; c) \equiv Q_t(^A Z; c) - Q_t(\text{core}), \quad (1)$$

where c stands for the configuration of the band in the nucleus $^A Z$ and $Q_t(\text{core})$ is the transition quadrupole moment of the assumed core nucleus. According to the “additivity principle” proposed in Ref. [27] (see also Ref. [28]), the quadrupole moment δQ_t can be expressed as a sum of individual contributions carried by individual particle and hole states which appear near the Fermi level. Namely, the relative transition quadrupole moment can be very well approximated by the “extreme shell model” expression

$$\delta Q_t \approx \delta Q_t^{\text{SM}} = \sum_i q_t(i), \quad (2)$$

where i runs over the particles and holes with respect to the core configuration in the nucleus $^A Z$. The quantity $q_t(i)$ represents the effective single-particle transition quadrupole moment, i.e., the change of the total intrinsic moment which is induced on the whole nucleus by the given particle or hole. By measuring or calculating values of $Q_t(^A Z; c)$ for a number of nuclei and configurations, one can extract values of $q_t(i)$ hence the quadrupole polarizabilities associated with individual orbitals.

The transition quadrupole moments for various highly-deformed structures in the $A\sim 135$ region have been measured in separate past experiments using the Doppler-shift attenuation method (DSAM), however conclusive comparisons between similar structures in different nuclei were limited because of systematic differences such as reaction choice and target retardation

properties. Specifically, the differences in the parameterization of the nuclear and electronic stopping powers, which act as an “internal clock” in DSAM measurements, have contributed to large variations in the extracted Q_t values reported for exactly the same nucleus and band. The absence of adequate experimental information on the time structure of the quasi-continuum side feeding contribution also provided additional uncertainty. In the present study, these systematic uncertainties were greatly reduced because a variety of different nuclei were produced under similar conditions and then analyzed using the same techniques. Furthermore, the high efficiency and resolving power of GAMMASPHERE coupled with Microball made it possible to explore the time structure of the side-feeding into particular bands.

3. Measurements

In this study, high-spin states of a variety of $A \sim 135$ nuclei ($Z=58-62$) were populated after fusion of a ^{35}Cl beam with an isotopically enriched 1 mg/cm^2 thick ^{105}Pd foil mounted on a 17 mg/cm^2 Au backing. The 173 MeV ^{35}Cl beam was provided by the 88-Inch Cyclotron at the Lawrence Berkeley National Laboratory. The emitted γ -rays were collected using the GAMMASPHERE spectrometer [29] consisting of 97 Compton-suppressed HPGe detectors. The evaporated charged particles were identified with the Washington University Microball detector system [30] allowing a clean separation of the different charged-particle exit channels.

The centroid-shift Doppler-shift attenuation method [31] was used in several different ways. For the most intense bands, spectra were generated by summing gates on the cleanest, fully stopped transitions at the bottom of the band of interest and projecting the events onto the “forward” (31.7° and 37.4°) and “backward” (142.6° and 148.3°) axes. These spectra were then used to extract the fraction of the full Doppler shift, $F(\tau) (= \frac{E_\gamma(\theta) - E_0}{E_0 \beta' \cos(\theta)})$, for transitions within the band of interest, [$E_\gamma(\theta)$ is the centroid of the γ -ray energy distribution as measured in a detector at angle θ with respect to the beam direction, E_0 is the unshifted γ -ray energy, and β' is the mid-target recoil velocity]. In addition, for many bands double gates were set on in-band “moving” transitions in any ring of detectors and data were once again incremented into separate spectra for events detected at “forward”, “90°”, and “backward” angles. For the most intense bands, Doppler-shifted coincidence gates could also be set on the highest spin transitions within the band, making it possible to eliminate the effect of side-feeding for states lower in the cascade. Approximately a 10% increase in the deduced quadrupole moment was found for the $i_{13/2}$ neutron configurations when using the latter method compared to the value extracted by gating on the stopped

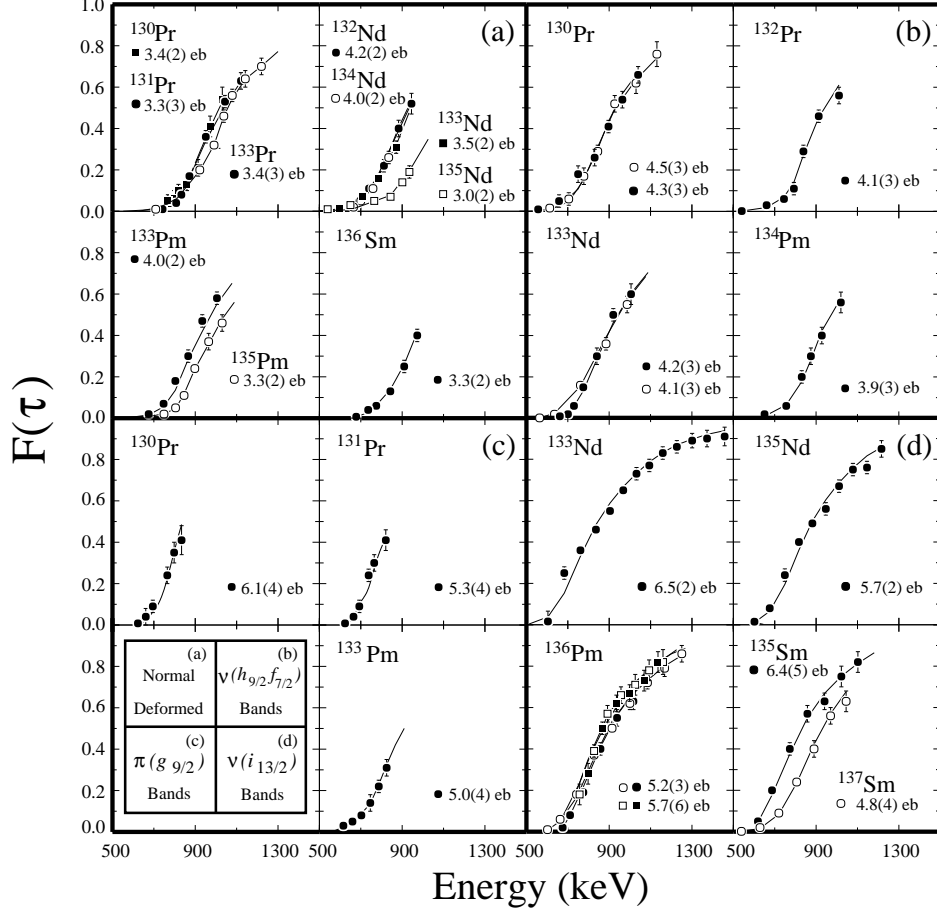


Fig. 1. Global $F(\tau)$ curves for some of the (a) normal deformed, (b) $\nu f_{7/2} h_{9/2}$, (c) $\pi g_{9/2}$, and (d) $\nu i_{13/2}$ bands measured in this work. Extracted quadrupole moment values are also given.

transitions at the bottom of the same band, which is in agreement with recent $^{131,132}\text{Ce}$ results [22]. A sample of these results is presented in Fig. 1.

In order to extract the intrinsic quadrupole moments from the experimental $F(\tau)$ values, calculations using the code FITFAU [32] were performed. The $F(\tau)$ curves were generated under the assumption that the band has a constant Q_t value. Although the uncertainties in the stopping powers and the modeling of the side-feeding may contribute an additional systematic error of 15–20% in the absolute Q_t values, the relative values are considered to be accurate to a level of 5–10%. Such precision allows

Table 1. Transition quadrupole moments measured in this work. Unless stated otherwise, Q_t values were deduced assuming $Q_t(\text{side feeding})=Q_t$. The stopping power uncertainties may contribute an additional systematic error of 10-15% in the absolute Q_t values.

Nucleus	Configuration ^a	$Q_t(\text{eb})$
¹³⁰ Pr	$\pi h_{11/2} \otimes \nu d_{5/2}$	3.4(2)
	$\pi h_{11/2} \otimes \nu(f_{7/2}, h_{9/2})$ (band 1)/(band 2)	4.3(3)/4.5(3)
¹³¹ Pr	$\pi g_{9/2} \otimes \nu h_{11/2}$	6.1(4)
	$\pi h_{11/2}$	3.3(3)
	$\pi g_{9/2}$	5.3(4)
¹³² Pr	$\pi h_{11/2} \otimes \nu(f_{7/2}, h_{9/2})$	4.1(3)
	$\pi g_{9/2} \otimes \nu i_{13/2}$	7.0(7)
¹³³ Pr	$\pi h_{11/2}$	3.3(3)
¹³² Nd	$\pi h_{11/2}$	4.2(2)
¹³³ Nd	$\nu h_{11/2}$	< 3.0
	$\nu h_{11/2} \otimes \pi(h_{11/2})^2$	3.5(3)
	$\nu g_{7/2} (\alpha = +1/2)/(\alpha = -1/2)$	3.4(2)/3.5(2)
	$\nu(f_{7/2}, h_{9/2}) (\alpha = +1/2)/(\alpha = -1/2)$	4.2(3)/4.1(3)
	$\nu i_{13/2}$	5.8(2), 6.5(2) ^b
¹³⁴ Nd	$\pi h_{11/2}$	4.0(2)
¹³⁵ Nd	$\nu h_{11/2}$	< 3.0
	$\nu h_{11/2} \otimes \pi(h_{11/2})^2$	3.0(3)
	$\nu i_{13/2}$	5.1(2), 5.7(2) ^b

^a $\pi g_{9/2}$: $9/2^+[404]$, $\pi h_{11/2}$: $3/2^- [541]$, $\pi d_{5/2}$: $3/2^+[411]$, $\nu h_{11/2}$: $7/2^- [523]$ and $9/2^- [514]$, $\nu g_{7/2}$: $7/2^+[404]$, $\nu d_{5/2}$: $5/2^+[402]$, $\nu(f_{7/2}, h_{9/2})$: $1/2^- [541]$, $\nu i_{13/2}$: $1/2^+[660]$.

^bDeduced by gating above the level of interest, so that side-feeding was eliminated. One may reasonably expect a similar increase of $\sim 10\%$ for the other highly-deformed bands listed [33].

a clear differentiation between the quadrupole polarizability of different orbital configurations for a variety of N and Z values, see Fig 2 and Ref.[41].

The present results, displayed in Table 1, especially when taken together with values for ^{131,132}Ce [22], extracted using an identical analysis procedure, clearly indicate that for structures involving the $\nu i_{13/2}$ orbital there is a systematic decrease in the deformation as a function of increasing proton and neutron numbers, see Fig 2.

Another important finding involves the highly-deformed bands built

Table 1. Continued.

Nucleus	Configuration ^a	Q_t (eb)
¹³³ Pm	$\pi h_{11/2}$	4.0(2)
	$\pi d_{5/2}$	4.1(2)
	$\pi g_{9/2}$	5.0(4)
¹³⁴ Pm	$\pi h_{11/2} \otimes \nu h_{11/2}$	3.3(2)
	$\pi h_{11/2} \otimes \nu(f_{7/2}, h_{9/2})$	3.9(2)
¹³⁵ Pm	$\pi h_{11/2}$	3.3(2)
	$\pi d_{5/2}$	3.5(2)
¹³⁶ Pm	$\pi h_{11/2} \otimes \nu h_{11/2}$	< 3.0
	$\pi h_{11/2} \otimes \nu i_{13/2}$ (band 1)	4.8(3), 5.2(3) ^b
	$\pi h_{11/2} \otimes \nu i_{13/2}$ (band 2)	4.8(4), 5.2(4) ^b
	$\pi g_{7/2} \otimes \nu i_{13/2}$ (band 1)	5.7(6)
	$\pi g_{7/2} \otimes \nu i_{13/2}$ (band 2)	5.7(6)
¹³⁵ Sm	$\nu i_{13/2}$	5.8(4), 6.4(4) ^c
¹³⁶ Sm	$\nu(h_{11/2})^2 \otimes \pi(h_{11/2})^2$	3.3(2)
¹³⁷ Sm	$\nu i_{13/2}$	4.4(3), 4.8(4) ^b

^a $\pi g_{9/2}$: $9/2^+$ [404], $\pi h_{11/2}$: $3/2^-$ [541], $\pi d_{5/2}$: $3/2^+$ [411], $\nu h_{11/2}$: $7/2^-$ [523] and $9/2^-$ [514], $\nu g_{7/2}$: $7/2^+$ [404], $\nu d_{5/2}$: $5/2^+$ [402], $\nu(f_{7/2}, h_{9/2})$: $1/2^-$ [541], $\nu i_{13/2}$: $1/2^+$ [660].

^bDeduced by gating above the level of interest, so that side-feeding was eliminated. One may reasonably expect a similar increase of $\sim 10\%$ for the other highly-deformed bands listed [33].

^cAssumed that the sidefeeding time structure was similar to other highly-deformed $\nu i_{13/2}$ bands where the $\tau_{sf} \sim 1.2\tau_{band}$.

upon the $9/2^+$ [404] ($g_{9/2}$) proton orbital in ^{130,131}Pr and ¹³³Pm [15, 17, 34]. Our results confirm the important role played by the $\pi g_{9/2}$ [404] $9/2^+$ hole orbitals in building highly-deformed structures in this region. It is seen in Fig 2 and Table 1 that the largest deformations are observed for the Ce isotopes ($Z=58$) where the $9/2^+$ [404] orbital lies above the Fermi surface [18].

It is also of interest to see by how much the strongly downsloping $1/2^-$ [541] ($f_{7/2}, h_{9/2}$) neutron orbital polarizes the nucleus towards an “enhanced” deformation. The trends for this orbital, which has Q_t values intermediate between the highly-deformed ($\nu i_{13/2}$ and $\pi g_{9/2}$) and normal deformed configurations, also seems to exhibit slightly decreasing Q_t values as a function of increasing Z . The normal deformed structures which dom-

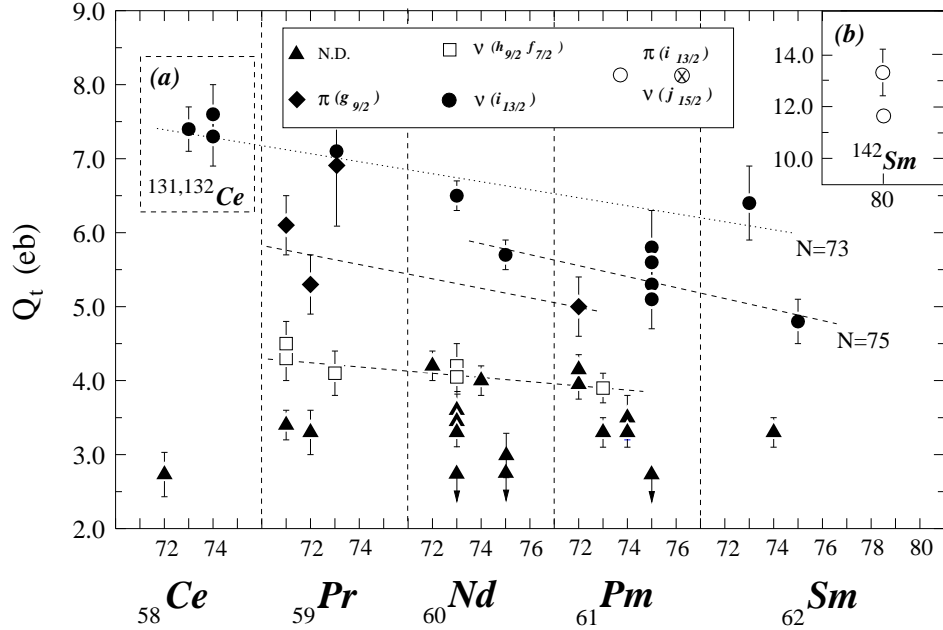


Fig. 2. Plot, as a function of Z and N , summarizing the quadrupole moments, Q_t extracted from this experiment. Quadrupole moments for the (a) highly-deformed bands in $^{131,132}\text{Ce}$ [22] and (b) the superdeformed bands in ^{142}Sm [25] using similar target and Au backing composition together with the same analysis procedures and stopping powers as the current work.

inate the yrast lines of these nuclei for low spin values, display Q_t values distinctly lower than the above mentioned configurations, with a generally constant trend as a function of Z and N . However, since these normal deformed structures are predicted to be extremely γ -soft and strongly influenced by pairing correlations, one has to exercise caution when interpreting trends in terms of single-particle occupations.

4. Theoretical Calculations and Differential Q_t Values

To obtain quantitative understanding of measured quadrupole moments, we performed systematic cranking calculations without pairing using two different self-consistent mean-field methods, namely the cranked Skyrme Hartree-Fock method (CSHF) (code HFODD [35]) with the Skyrme parameterization SLy4 [36], and the cranked relativistic mean-field theory (CRMF) [37, 40] with the parameterization NL1 [38]. Both methods have shown to provide an accurate description of various properties of rotational

Table 2. Effective charge quadrupole moments q_{20} (in eb) for single-particle orbitals around ^{131}Ce core. The values were extracted from the set of 183 calculated bands in CSHF and 105 bands in CRMF. The orbitals are labeled by means of asymptotic quantum numbers $[Nn_z\Lambda]\Omega$ and the signature quantum number α (the subscripts \pm stand for $\alpha=\pm 1/2$). Note that in most cases the signature dependence is very weak (as observed in experiment, see Table 1).

Orbital	CSHF	CRMF	Orbital	CSHF	CRMF
Neutrons			Protons		
$[402]_{\frac{5}{2}-}$	-0.35	-0.26	$[404]_{\frac{9}{2}-}$	-0.32	-0.37
$[402]_{\frac{5}{2}+}$	-0.33	-0.26	$[404]_{\frac{9}{2}+}$	-0.32	-0.37
$[411]_{\frac{1}{2}-}$	-0.15	-0.11	$[422]_{\frac{3}{2}-}$	0.33	0.33
$[411]_{\frac{1}{2}+}$	-0.12	-0.06	$[422]_{\frac{3}{2}+}$	0.34	0.28
$[411]_{\frac{3}{2}-}$	-0.15	-0.13	$[532]_{\frac{5}{2}-}$	0.43	0.41
$[411]_{\frac{3}{2}+}$	-0.11	-0.12	$[532]_{\frac{5}{2}+}$	0.56	0.54
$[413]_{\frac{5}{2}-}$	-0.13	-0.13	$[541]_{\frac{3}{2}-}$	0.50	0.48
$[413]_{\frac{5}{2}+}$	-0.12	-0.11	$[541]_{\frac{3}{2}+}$	0.57	0.50
$[523]_{\frac{7}{2}-}$	0.03	0.05	$[550]_{\frac{1}{2}+}$	0.49	0.47
$[523]_{\frac{7}{2}+}$	0.04	0.01			
$[530]_{\frac{1}{2}-}$	0.22	0.17			
$[530]_{\frac{1}{2}+}$	0.17	0.19			
$[532]_{\frac{5}{2}-}$	0.19	0.17			
$[532]_{\frac{5}{2}+}$	0.24	0.38			
$[541]_{\frac{1}{2}-}$	0.35	0.35			
$[541]_{\frac{1}{2}+}$	0.37	0.33			
$[660]_{\frac{1}{2}+}$	0.38	0.40			
$[660]_{\frac{1}{2}-}$	0.36	0.36			

bands in different mass regions (see, e.g., Refs. [27, 39, 40, 10]). For the details pertaining to theoretical calculations, see the forthcoming Ref. [42].

For the reference band, we took the lowest highly deformed $\nu(i_{13/2})$ intruder band in ^{131}Ce . According to calculations [14], large deformed energy gaps develop at high angular momentum for $Z=58$ and $N=73$, i.e., ^{131}Ce can be considered as a (super)deformed core in the $A\sim 135$ mass region. In order to perform a reliable statistical analysis of individual quadrupole moments according to Ref. [27], it was necessary to carry out calculations for a large number of nuclei and configurations: our data set consisted of over 100 bands in both CSHF and CRMF calculations.

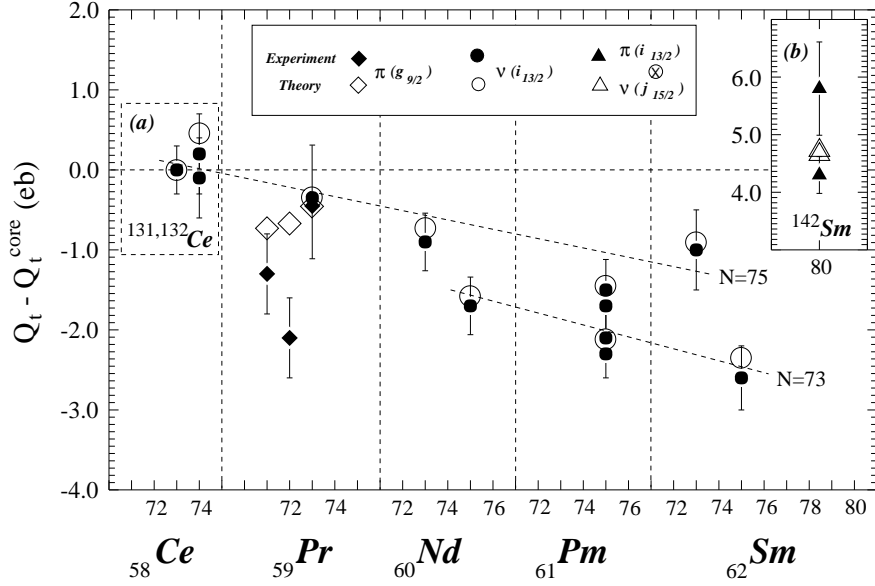


Fig. 3. Experimental (closed symbols with error bars) and calculated (CSHF; open symbols) differential transition quadrupole moments (equation 1) for a number of nuclei from the $A \sim 135$ mass region. The highly-deformed band in ^{131}Ce (containing one $i_{13/2}$ neutron and two $g_{9/2}$ proton holes) was used as a reference core configuration. The data for $^{131,132}\text{Ce}$ were taken from Ref. [22]. The corresponding values for ^{142}Sm (see Ref. [25] for experimental data) are shown in the inset. It is to be noted that for the differential quadrupole moments the problem with the stopping-power uncertainties is less severe. For comparison with Fig. 2, the calculated value of Q_t for the ^{131}Ce core configuration was 7.75 eb in CSHF and 7.57 eb in CRMF.

Within the cranking model, the transition quadrupole moment can be written as [43]

$$Q_t = Q_{20} + \sqrt{\frac{2}{3}}Q_{22}, \quad (3)$$

where Q_{20} and Q_{22} are calculated components of the quadrupole moment. (Let us note that due to the non-standard normalisation of Q_{22} in Ref. [35], one gets $Q_{22}(\text{Ref. [35]}) = -\sqrt{2}Q_{22}$.) Figure 3 shows the experimental and calculated (CSHF) values of Q_t relative to a ^{131}Ce core, for the highly deformed bands in nuclei with $Z=57-62$ involving $i_{13/2}$ neutrons and/or $g_{9/2}$ proton holes. The agreement between experiment and theory is quite remarkable, with all the major experimental trends discussed previously being well reproduced.

From the differential proton quadrupole moments δQ_{20}^π and δQ_{22}^π calculated at rotational frequency of $\hbar\omega=0.65$ MeV, effective single-particle charge quadrupole moments $q_{20}(i)$ and $q_{22}(i)$ were extracted for protons and neutrons according to the additivity principle, Eq. (2). Of course, $q_t(i) = q_{20}(i) + \sqrt{\frac{2}{3}}q_{22}(i)$ are the effective values for the single-particle/hole states. The results of our linear regression analysis for q_{20} are displayed in Table 2. (For tabulated values of q_{22} and angular momentum alignments, see Refs. [42].) It is seen that the two models give very similar results. In particular, quadrupole polarizabilities of the lowest $i_{13/2}$ neutron orbitals, [541]1/2 neutron orbitals, and $g_{9/2}$ proton holes are comparable. The fact that the bands attributed to the [541]1/2 neutron orbital are experimentally significantly less deformed than the $i_{13/2}$ intruder structures can probably be attributed to pairing correlations which effectively reduce the occupation of [541]1/2. With these values at hand one can calculate quadrupole moments Q_{20} for near-axial bands in the $A\sim 135$ mass region.

The general trend of decreasing Q_t in the highly-deformed structures with increasing Z and N , see Fig. 3, is consistent with general expectations that as one adds particles above a deformed shell gap, the stabilizing effect of the gap may be diminished. This trend continues until a new “magic” deformed number is reached. Such an event clearly occurs from ^{132}Ce to higher N and Z until $Z=62$ and $N=80$ (^{142}Sm) where a large jump in quadrupole moment occurs marking the point at which it becomes energetically favorable to fill the high- j $\pi i_{13/2}$ and $\nu j_{15/2}$ orbitals creating the $A\sim 142$ superdeformed island, see the inset in Fig. 3. It is gratifying to see that theory can reproduce the Q_t in ^{142}Sm using *both* ^{131}Ce and ^{152}Dy cores.

5. Summary and Conclusions

In summary, it has been possible to extract differential transition quadrupole moments, free from common systematic errors for over 15 different nuclei at high spin within a single experiment. This comprehensive study establishes Z , N , and configuration dependent quadrupole moment trends in the $A\sim 135$ light rare-earth region. Detailed comparisons are made with theoretical calculations using the Cranked Hartree-Fock and Cranked Relativistic Mean Field frameworks. Theoretical differential transition quadrupole moments agree very well with experimental data for highly deformed intruder bands in this region. Based on the additivity principle, valid in the limit of weak residual correlations, the effective single-particle charge quadrupole moments have been obtained. Together with values of Ref. [27] around ^{152}Dy , they can be used to estimate the quadrupole moments of specific near-axial configurations in a wide range of nuclei.

Discussions with R.V.F. Janssens, D. Ward, and A. Galindo-Uribarri are acknowledged and greatly appreciated. Special thanks to D.C. Radford and H.Q. Jin for software support, and to R. Darlington for help with the target. The authors wish to extend their thanks to the staff of the LBNL GAMMASPHERE facility for their assistance during the experiment. This work was supported in part by the U.S. Department of Energy under Contract Nos. DE-FG02-96ER40963 (University of Tennessee), DE-FG05-87ER40361 (Joint Institute for Heavy Ion Research), and DE-AC05-00OR22725 with UT-Battelle, LLC (Oak Ridge National Laboratory), the National Science Foundation, the State of Florida, the U.K. Engineering and Physical Science Research Council, the U.K. Council for the Central Laboratory of the Research Councils, and the Polish Committee for Scientific Research (KBN). MAR and JS acknowledge the receipt of a NATO Collaborative Research Grant. A.V.A. acknowledges support from the Alexander von Humboldt Foundation.

REFERENCES

- [1] H.B.G. Casimir, On the Interaction Between Atomic Nuclei and Electrons, Prize Essay, Teyler's, Tweede, Haarlem. [II:2],(1936).
- [2] N. Bohr and F. Kalckar, Mat. Fys. Medd. Dan. Vid. Selsk. 14, No. 10 (1937) or *Niels Bohr's Collected Work* **Vol. 9**, North Holland Publishing Company, Amsterdam (1985).
- [3] A. Bohr and B.R. Mottelson, *Nuclear Structure* (Benjamin, New York, 1975), Vol. II.
- [4] Z. Szymanski, *Fast Nuclear Rotation* (Clarendon Press,Oxford,1983).
- [5] S.G. Nilsson and I. Ragnarsson, *Shapes and Shells in Nuclear Structure* (Cambridge University Press, Cambridge, 1995).
- [6] H.A. Jahn and E. Teller, Proc. R. Soc. London, Ser. A **161**, 220 (1937).
- [7] A. Bohr, Mat. Fys. Medd. Dan. Vid. Selsk. 26, No. 14 (1952).
- [8] P.-G. Reinhard and E.W. Otten, Nucl. Phys. **A420**, 173 (1984).
- [9] W. Nazarewicz, Int. J. Mod. Phys. **E2**, 51 (Supp. 1993); Nucl. Phys. A **A574**, 27c (1994).
- [10] A.V. Afanasjev, I. Ragnarsson, and P. Ring, Phys. Rev. C **59**, 3166 (1999).
- [11] A.V. Afanasjev, D.B. Fossan, G.J. Lane, and I. Ragnarsson, Phys. Rep. **322**, 1 (1999)
- [12] G. de France, C. Baktash, B. Haas, and W. Nazarewicz, Phys. Rev. C **53**, R1070 (1996)
- [13] R.B. Firestone, B. Singh, and S.Y.F. Chu, *Table of Superdeformed Nuclear Bands and Fission Isomers*, (1997).
- [14] R. Wyss *et al.*, Phys. Lett. B **215**, 211 (1988).

- [15] A. Galindo-Uribarri *et al.*, Phys. Rev. C **50**, R2655 (1994).
- [16] F.G. Kondev *et al.*, J. Phys. **G25**, 893 (1999).
- [17] A. Galindo-Uribarri *et al.*, Phys. Rev. C **54**, 1057 (1996).
- [18] A.V. Afanasjev and I. Ragnarsson, Nucl. Phys. **A608**, 176 (1996).
- [19] F.G. Kondev *et al.*, Phys. Rev. C. **59**, 3076 (1999).
- [20] F. Lerma *et al.*, Phys. Rev. Lett. **83**, 5447 (1999).
- [21] P. Regan *et al.*, J. Phys. **G18**, 847 (1992).
- [22] R.M. Clark *et al.*, Phys. Rev. Lett. **76** (1996).
- [23] H. Savajols *et al.*, Phys. Rev. Lett. **76**, 4480 (1996).
- [24] D. Nisius *et al.*, Phys. Lett. **B392**, 18 (1997).
- [25] G. Hackman *et al.*, Phys. Lett. B **416**, 268 (1998).
- [26] B.C. Busse *et al.*, Phys. Rev. C **57**, R1017 (1998).
- [27] W. Satuła, J. Dobaczewski, J. Dudek, and W. Nazarewicz, Phys. Rev. Lett., **77**, 5182 (1996).
- [28] L.B. Karlsson, I. Ragnarsson, and S. Åberg, Phys. Lett. B **416**, 16 (1998); Nucl. Phys. A **639**, 654 (1998)
- [29] R.V.F. Janssens and F.S. Stephens, Nucl. Phys. News **6**, 9 (1996).
- [30] D.G. Sarantites *et al.*, Nucl. Instrum. Methods Phys. Res **A381**, 418 (1996).
- [31] T.K. Alexander and J.S. Forster, *Advances in Nuclear Physics*, edited by M. Baranger and E. Vogt (Plenum, New York 1978), Vol.10, p197.
- [32] E.F. Moore *et al.*, in *Proceeding of the Conference on Nuclear Structure at the Limits, Argonne, Illinois, 1996*, (ANL/PHY-97/1) p.72.
- [33] F.G. Kondev *et al.*, Phys. Rev. C **60**, 011303 (1999).
- [34] T.B. Brown *et al.*, Phys. Rev. C **56**, R1210 (1997).
- [35] J. Dobaczewski and J. Dudek, Comp. Phys. Comm. **131**, 164 (2000).
- [36] E. Chabanat *et al.*, Nucl. Phys. **A635**, 231 (1998).
- [37] W. Koepf and P. Ring, Nucl. Phys. A **493**, 61 (1989); and A **511**, 279 (1990)
- [38] P.-G. Reinhard *et al.*, Z. Phys. A **323**, 13 (1986).
- [39] N.El Aouad *et al.*, Nucl. Phys. A **676**, 155 (2000).
- [40] A.V. Afanasjev, J. König, and P. Ring, Nucl. Phys. A **608**, 107 (1996).
- [41] R.W. Laird *et al.*, submitted.
- [42] M. Matev *et al.*, in preparation.
- [43] P. Ring *et al.*, Phys. Lett. B **110**, 423 (1982).